Interaction of Surface Radiation with Convection in Crystal Growth by Vapor Transport

Mohammad Kassemi* and Walter M. B. Duval†
NASA Lewis Research Center, Cleveland, Ohio 44135

Growth of single crystals from vapor in closed ampoules is governed by an intricate interplay between mass, momentum, and heat transfer processes. The objective of this study is to examine and isolate the effects of surface radiation heat transfer on the vapor transport process using a mathematical model. The model consists of a set of coupled nonlinear partial differential equations for conservation of mass, momentum, energy, and species, and the integro-differential equations that represent radiative exchange. It depends on five important physical parameters. These are Grashof number, Prandtl number, Schmidt number, aspect ratio, and the radiation-conduction number. The effects of these dimensionless groupings are systematically investigated. From the cases examined, it is concluded that surface radiation can change the flow structure appreciably. This is especially true in microgravity environment where radiation competes primarily with conduction in modifying the thermal profiles. The numerical results also show that in the presence of radiation, the top-heating configuration (source on top) is no longer stable and that near the growing crystal, radiation-induced vortices can introduce significant nonuniformities in the growth flux.

Nomenclature

A	= surface area
AR	= aspect ratio, (L/H)
D_{AB}	= binary diffusivity
$(\partial^2 s_j s_i)/(\partial A_i \partial A_j)$	= exchange factor between differential areas i and j
g	= gravitational acceleration
g	= gravitational acceleration vector
Gr	= Grashof number, $[\beta g H^3 (T_s - T_c)/\nu^2]$
H	= height of the enclosure
L	= length of the enclosure
Nr	= radiation-conduction number, $[\sigma T_s^3 H/\lambda(1-\gamma)]$
Pr	= Prandtl number, (ν/α)
Sc	= Schmidt number, (ν/D_{AB})
t	= time
T	= temperature
u	= dimensionless velocity in the x direction, $[u^* H/\nu]$
u_c	= normal velocity at the crystal interference, $u(AR, y)$
v	= dimensionless velocity in the y-direction, $[v^* H/\nu]$
W_A	= weight fraction of component A
x, y	= dimensionless coordinates $[(x^*/H), (y^*/H)]$
α	= thermal diffusivity
β	= coefficient of thermal expansion
γ	= temperature ratio, (T_c/T_s)
θ	= dimensionless temperature $[(T - T_c)/(T_s - T_c)]$
λ	= thermal conductivity
ν	= coefficient of dynamic viscosity
σ	= Stefan-Boltzmann constant
φ	= inclination angle
ψ	= dimensionless stream function, (ψ^*/ν)
ω	= dimensionless vorticity, $[\omega^* H^2/\nu]$

Subscripts

c	= crystal interface
s	= source interface
1,2	= insulated side walls

Superscripts

c	= crystal interface
s	= source interface
*	= dimensional quantities

Introduction

In recent years, crystal growth from the vapor phase has found an increasingly important role in the preparation of insulators, metals, semiconductors, acousto-optic, and opto-electronic materials. Large single crystals and polycrystalline samples are typically grown in closed systems under an imposed temperature gradient. The nutrient sublimes from the source material at one end of the enclosure and diffuses to the crystal at the opposite end. This diffusive flow is also known as the Stefan wind. When significant density gradients are present in the vapor, a natural convective recirculating flow ensues. The convective flow can arise from molecular weight differences of the gaseous species (concentration gradients), commonly called solutal convection, and/or from thermal expansion (temperature gradients), frequently referred to as thermal convection. Since this flow is buoyancy driven, the magnitude and direction of the gravity vector are also important parameters of the problem. In short, it is seen that notwithstanding the relative simplicity of the crystal growth procedure, the underlying physical phenomena are quite complex and encompass the coupling effect of momentum, heat, and species transport. Although simplification is desirable to manage the multiplicity of the governing phenomena, there is also a considerable need for accurate prediction of the transport rates through rigorous analysis. It is noted that experiments conducted in space under low-gravity conditions produced results[1] that still defy quantitative interpretation.

The fluid dynamics of crystal growth is described in a comprehensive review by Rosenberger.[2] In recent years, numerous works have been reported on the theoretical formulation of the chemical and physical vapor transport processes (CVT and

Received March 3, 1989; revision received July 20, 1989.

*NRC-NASA Resident Researcher. Member AIAA.
†Physicist.

PVT, respectively). The pioneering work is due to Klosse and Ullersma (KU),[3] who obtained an analytical solution of the two-dimensional transport problem subject to rather stringent assumptions. Greenwell et al.[4] considered diffusive PVT, including viscous interaction with the walls. They neglected the effect of thermal and solutal convection and showed a diffusion-induced recirculation of the inert gas. Later, Jhaveri and Rosenberger[5] solved the transport equations subject to thermal convection and set a parametric limit to KU's model. Markham and Rosenberger[6] extended this analysis to inclined enclosures. In all of the above investigations except for KU, the normal interfacial velocity was related to local concentration gradients through Fick's law. More recently, Extremet et al.[7] studied the effects of simultaneous solutal and thermal convection in a multizonal rectangular enclosure. However, they introduced an a priori specified interfacial mass flux. Finally, Zappoli[8] extended previous work by considering the effect of interfacial kinetics on mass transfer in the PVT/CVT enclosure.

In recent years, it has been recognized[9] that when natural convection is the major mode of heat transfer in gases, radiation between surfaces plays a significant role. It has also been intuitively recognized that thermal radiation is an important factor in all materials processing. As pointed out by previous investigators,[2,6,10] this includes crystal growth from the vapor phase. However, to date, the effects of thermal radiation on the PVT/CVT processes have been left undisclosed.

The main objective of this work is, therefore, to study the effect of thermal radiation on the transport process during vapor phase crystal growth. Interaction of radiation with convection in general can be classified into two modes. The first is the passive interaction in which radiation exchange takes place only between the boundary surfaces. The second is the active interaction where the vapor also participates in the radiative transfer. In this work, we are only concerned with passive interaction, exemplified by opaque crystals growing in opaque crucibles with the vapor transparent to radiation. Our goal is to show that surface radiative exchange can significantly alter the temperature distribution and the flow structure in the vapor, especially in the low-gravity environment where radiation easily can be the dominant heat transfer mode.

Mathematical Formulation

Following KU's model, we consider a cavity of height H and length L. The cavity is inclined at an angle of φ with respect to the gravity vector as depicted in Fig. 1. As in the classical vapor transport problem, a source of solid A at a temperature T_s forms one side of the enclosure whereas the crystal (sink) at temperature T_c occupies the opposite end. The interfaces are assumed to be flat. With $T_s > T_c$, component A sublimes from the source, transports through and with a nonreacting component B, and condenses at the crystal interface. W_A^s and W_A^c are, respectively, the weight fractions of component A in equilibrium with the solid interfaces. Vertical boundary temperatures T_s and T_c are uniform. The horizontal boundaries are insulated. In the passive mode, the vapor is assumed to be transparent to thermal radiation. Therefore, in the energy balance for the vapor, radiative contributions are neglected. Radiation effects are, however, introduced at the boundaries where radiative transfer is balanced by convection. To simplify the analysis, all boundaries are assumed to be black. Furthermore, since we are interested only in thermal convection, the molecular weights of the two vapor components are assumed to be the same.

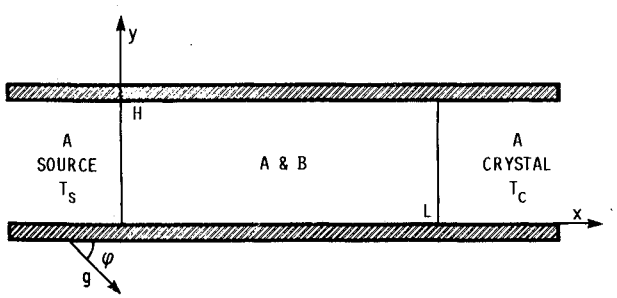

Fig. 1 Vapor transport enclosure.

Transport in the cavity is governed by a system of nonlinear coupled conservation equations for mass, momentum, species, and energy. The flow is laminar. The radiative boundary conditions are represented by integro-differential equations. Using the stream function-vorticity formulation and invoking the Boussinesq approximation, the governing equations are cast into the following dimensionless form.

Momentum equation:

$$\frac{\partial \omega}{\partial t} + u\frac{\partial \omega}{\partial x} + v\frac{\partial \omega}{\partial y} = \frac{\partial^2 \omega}{\partial x^2} + \frac{\partial^2 \omega}{\partial y^2} + Gr\left(\frac{\partial \theta}{\partial x}\sin\varphi + \frac{\partial \theta}{\partial y}\cos\varphi\right) \quad (1)$$

where

$$u = \frac{\partial \psi}{\partial y}, \qquad v = -\frac{\partial \psi}{\partial x} \quad (2)$$

$$\frac{\partial^2 \psi}{\partial x^2} + \frac{\partial^2 \psi}{\partial y^2} = -\omega \quad (3)$$

subject to the following boundary conditions:

$$u = -\frac{1}{Sc}\left[(\partial W_A/\partial x)/(1 - W_A)\right], \qquad v = 0$$

$$\text{for} \quad x = 0, \quad A\,0 \le y \le 1 \quad (4)$$

$$u = v = 0 \quad \text{for } y = 0,1 \quad 0 \le x \le A \quad (5)$$

Species equation:

$$\frac{\partial W_A}{\partial t} + u\frac{\partial W_A}{\partial x} + v\frac{\partial W_A}{\partial y} = \frac{1}{Sc}\left(\frac{\partial^2 W_A}{\partial x^2} + \frac{\partial^2 W_A}{\partial y^2}\right) \quad (6)$$

subject to

$$W_A = W_A^s, W_A^c \qquad \text{for} \qquad x = 0, A \qquad 0 \le y \le 1 \quad (7)$$

$$\frac{\partial W_A}{\partial y} = 0 \qquad \text{for} \qquad y = 0,1 \qquad 0 \le x \le A \quad (8)$$

Energy equation:

$$\frac{\partial \theta}{\partial t} + u\frac{\partial \theta}{\partial x} + v\frac{\partial \theta}{\partial y} = \frac{1}{Pr}\left(\frac{\partial^2 \theta}{\partial x^2} + \frac{\partial^2 \theta}{\partial y^2}\right) \quad (9)$$

subject to

$$\theta = 1,0 \qquad \text{for} \qquad x = 0, A \qquad 0 \le y \le 1 \quad (10)$$

$$\theta = \theta_1, \theta_2 \qquad \text{for} \qquad y = 0,1 \qquad 0 \le x \le A \quad (11)$$

where temperatures θ_1 and θ_2 are given by a balance between conduction and radiation at the wall as:

$$\frac{\partial \theta_1}{\partial y} = Nr\left\{\left[\left(1-\gamma\right)\theta_1 + \gamma\right]^4 - \int_{A_s} \frac{\partial^2 S_s S_1}{\partial A_1 \partial A}\, dA - \int_{A_c} \gamma^4 \frac{\partial^2 S_c S_1}{\partial A_1 \partial A}\, dA - \int_{A_2}\left[\left(1-\gamma\right)\theta_2 + \gamma\right]^4 \frac{\partial^2 S_2 S_1}{\partial A_1 \partial A}\, dA\right\} \quad (12)$$

$$-\frac{\partial\theta_2}{\partial y} = Nr\left\{\left[\left(1-\gamma\right)\theta_2+\gamma\right]^4 - \int_{A_s}\frac{\partial^2 s_s s_2}{\partial A_2 \partial A}\,dA - \int_{A_c}\gamma^4\frac{\partial^2 s_c s_2}{\partial A_2 \partial A}\,dA - \int_{A_1}\left[\left(1-\gamma\right)\theta_1+\gamma\right]^4\frac{\partial^2 s_1 s_2}{\partial A_2 \partial A}\,dA\right\} \quad (13)$$

The dimensionless groups Gr, Sc, Pr, $\mathcal{R}$, Nr, and γ are described in the nomenclature. The most unfamiliar term is perhaps the radiation-conduction number Nr, which is defined as the ratio of radiation heat transfer to conduction heat transfer. Note that in the limit $Nr \to 0.0$, a pure convective situation is approached, and as Nr increases, the contribution of radiation is intensified.

A few of the underlying assumptions merit a brief discussion. The nonslip boundary conditions in Eq. (5) have been subject to some controversy. However, for equal molecular weights any diffusion slip can be safely neglected.[4,6] Simultaneous use of the nonslip conditions and the interfacial diffusion velocities of Eq. (4) give rise to mathematical singularities at the four corners of the cavity. Fortunately, as has been previously discussed by other investigators,[5,6] these discontinuities appear to have little effect on the final solutions, especially in the parametric range of interest. In vapor growth, the assumption of stationary interfaces is acceptable, since in general the rate at which the interface moves is orders of magnitude smaller than the flow velocities. To assume planar interfaces, however, may be far removed from reality; since, as will be shown, both convection and surface radiation can contribute to significant nonuniformities in the growth flux. The assumption of black surfaces is acceptable for quartz glass that absorbs most of the blackbody radiation emitted by sources below 1000 K. Different crystalline materials, however, have different surface radiative properties; here, black boundaries represent a general, if simplified, behavior. In spite of these simplifying assumptions, since the purpose of this paper is to point out useful trends, we hope that the semiquantitative guidance obtained from our results will be useful for the practitioners, until more rigorous treatments can be carried out.

Numerical Formulation

In order to solve the system of nonlinear, coupled partial differential equations, a staggered grid described by Wong and Raithby[11] was used. Note that in a staggered mesh, the stream function nodes form a cell. At the center of this cell, the vorticity, concentration, and temperature nodes are specified. The conservation equations were discretized by the conservative QUICK scheme that is due to Leonard.[12]

Radiative transfer was represented using the zonal approach.[13,14] It consists of dividing the solid boundaries into surface zones or elements. Elemental temperature distributions (in our case linear) are assumed within the zones in terms of local coordinates and nodal temperatures. In this fashion, radiative exchange can be described in terms of summations of direct exchange integrals.[13] These quantities are tabulated a priori for a given cavity geometry and then used during the numerical simulation as known coefficients.

The time-dependent finite-difference equations were integrated from arbitrary initial values (one-dimensional solutions) and steady-state solutions were arrived at by marching through time. The QUICK scheme is nominally third-order accurate in space; the vorticity boundary conditions were determined in a manner consistent with the overall accuracy of the scheme.[12] By using a quadratic upwind interpolation, the method enjoys feedback stability while at the same time it does not suffer from numerical diffusion inaccuracies caused by second derivative truncation terms of first-order upwind schemes. In the limiting case of natural convection in a square enclosure, we compared our results for velocity, stream function, temperature, and Nusselt number (for 20×20 and 40×40 grids) with benchmark solutions provided by De Vahl Davis,[15] and agreement was found to be excellent. The zonal scheme conserved radiative energy up to 1×10^{-6}. Its integrity was verified through comparison with limiting solutions available in the literature. The computer program was vectorized to fully exploit the power of CRAY XMP.

Results and Discussion

During the course of this investigation, many different cases were examined. For the sake of brevity, we limit the results presented here to two basic configurations, horizontal and vertical, and to a crystal growth process described by $W_A^s = 0.8$, $W_A^c = 0.7$, $Pr = 0.70$, $Sc = 1.0$, and $\mathcal{R} = 5$. First, we consider the horizontal enclosure where $\varphi = 90$ deg and the source and the crystal, respectively, form the left and right vertical boundaries. Here, the gravity vector acts perpendicular to the temperature difference. Second, we consider the vertical configuration where $\varphi = 0$ deg. In this case, the source and the crystal, respectively, form the top and bottom boundaries, and the gravity vector is parallel to the imposed temperature difference. Most of the results were generated using a 32×16 mesh. Details of the flow were satisfactorily resolved by the grid, and further refinement of the mesh did not produce more accurate results.

Horizontal Enclosure

This situation is also referred to as the unstable configuration because when the temperature difference is imposed, a natural convection recirculating flow known as conventional convection ensues. We first examine conditions that are relevant to the microgravity environment of space. In this case, temperature differences are significant so that radiative transfer can be important. But because of the reduced g level,

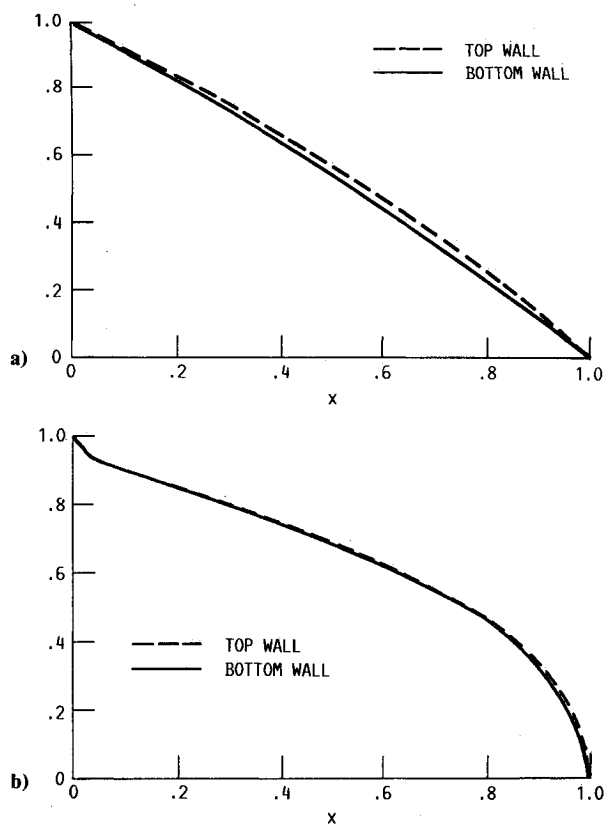

Fig. 2 Wall temperature distribution for $Gr = 700$; a) no radiation, $Nr \to 0.0$; b) radiation, $Nr = 7.0$.

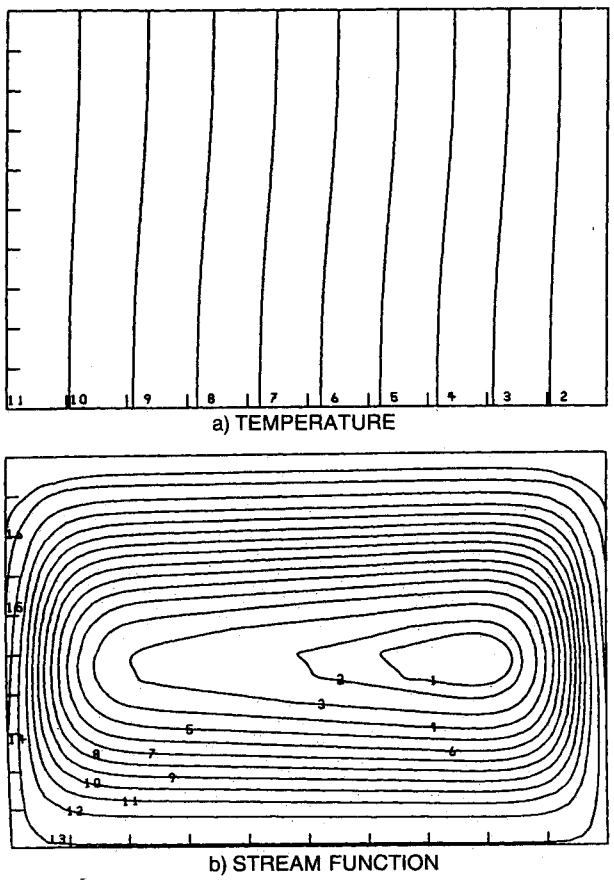

Fig. 3 Flow and temperature fields for $Gr = 700$ and $Nr \rightarrow 0.0$.

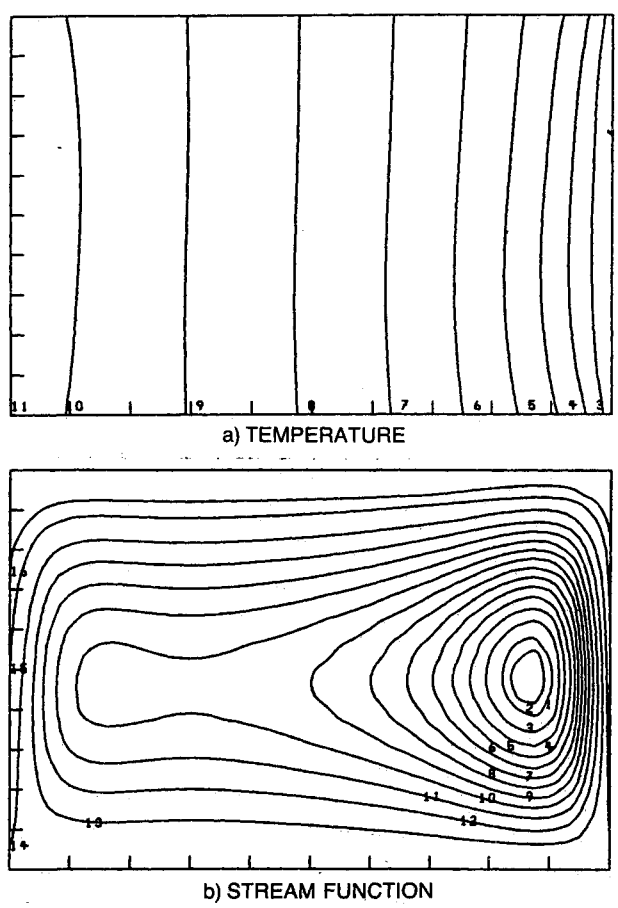

Fig. 4 Flow and temperature fields for combined convection and radiation heat transfer; $Gr = 700$, $Nr = 7.0$.

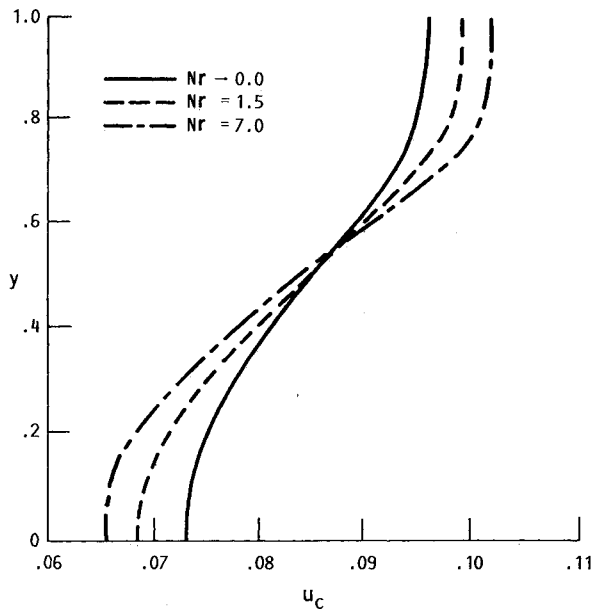

Fig. 5 Effect of the radiation-conduction number on the normal velocity distribution at the crystal interface for $Gr = 700$.

Grashof numbers are low, and therefore conduction is the mode of heat transfer in the vapor.

The results for $Gr = 700$, $\gamma = 0.50$, and Nr values of 0.0, 1.5, and 7.0 are shown in Figs. 2–5. In the passive mode, the influence of radiation is first felt at the boundaries. As shown in Fig. 2, in the absence of radiation ($Nr \rightarrow 0$), conduction is the dominant mode of heat transfer; therefore the wall temperature profiles are fairly linear. The top wall is at a slightly higher temperature because the hot fluid flows in the upper portion of the cavity, as will be seen later. When radiation effects are introduced, as for $Nr = 7$, the wall temperature distribution is drastically altered. Radiation emitted by the hot source is absorbed by the side walls. Consequently, side-wall temperatures increase, especially near the crystal interface. Note also that because of radiative exchange between the side walls, their temperature profiles are almost identical.

Next, we look at the flowfield. For $Nr \rightarrow 0$ there are no radiation effects, and as shown in Fig. 3, the vapor heated by the source rises, is forced down the cavity, and finally sinks as it is cooled at the crystal interface. A core-driven natural convective recirculating flow is therefore imposed on the purely diffusive Stefan wind. This means that the source and the crystal are more closely connected in the upper portion of the cavity. The normal velocity distributions at the crystal interface are shown in Fig. 5. Note that in the upper region where convection reinforces the flow, there is an increase in the interfacial flux, but in the bottom portion where the flow opposes the supply of nutrient, a much lower interfacial flux is attained. Needless to say, this asymmetry and nonuniformity is caused by convection, in the absence of which a symmetric and much more uniform interfacial velocity is predicted.

In the presence of radiation, the flow structure is significantly changed. Since the side-wall temperatures are increased by radiation as was previously discussed, extra heat is imparted to the fluid, especially near the crystal interface. At $Gr = 700$, the flow is not strong, and a substantial increase in the temperature gradients occurs near the growth interface to remove the added heat. This is clearly evident from a comparison of temperature contours in Figs. 3 and 4. The steeper gradients intensify the flow, and as shown in Fig. 4, a vigorous vortex is created near the crystal that would naturally increase the nonuniformity in the normal velocity distribution at the interface. Note from Fig. 5 that the extent of this nonuniformity increases as radiation effects are augmented by an increase in Nr values.

The effect of the temperature ratio γ on the normal velocity distribution at the interface is shown in Fig. 6 for $Gr = 700$ and $Nr = 7$. Note that for a fixed Nr, as γ approaches one, the nonuniformity caused by radiation decreases. This is intuitively expected, since radiative transfer decreases as temperature differences become smaller. In general, radiative transfer is controlled by the two dimensionless parameters Nr and γ. Our numerical results, as exemplified by Figs. 5 and 6, show

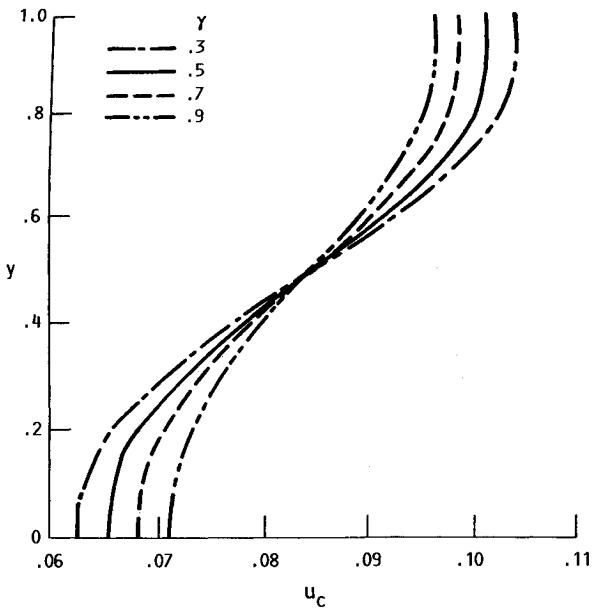

Fig. 6 Effect of temperature ratio on the normal velocity distribution at the crystal interface for $Gr = 700$, $Nr = 7.0$.

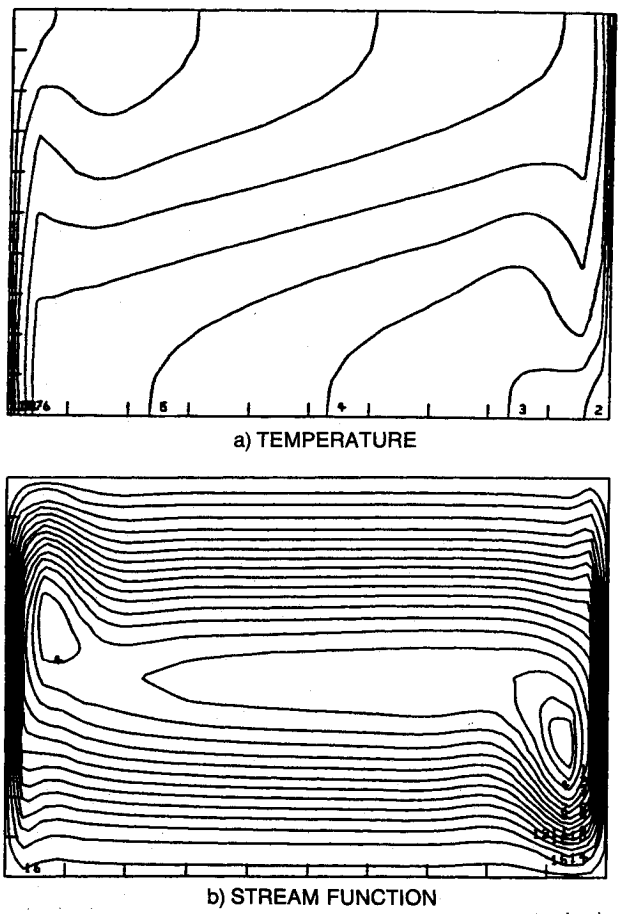

Fig. 7 Flow and temperature fields for $Gr = 1 \times 10^5$ and $Nr \rightarrow 0$.

that for low-to-moderate Nr values (below 10), radiation effects are important for γ at or below 0.80. At higher Nr values, however, radiation effects can be important even for γ above 0.80.

In the previous cases, the Gr numbers were relatively low. Therefore, radiation competed with conduction for controlling the heat transfer process. It is interesting to study the effect of radiation at Grashof numbers where convection is the dominant mode of heat transfer in the fluid. We examine the case of $Gr = 1 \times 10^5$ and $\gamma = 0.50$. First, consider $Nr = \rightarrow 0.0$ situation where radiation effects are neglected. Under these conditions, a strong convective flow exists in the enclosure. The stream function distribution in Fig. 7 indicates the existence of two recirculating cells, one near the source and the other near the crystal interface. The temperature contours of Fig. 7 indicate the formation of boundary layers near the two interfaces. Therefore, unlike the low Gr number case that was core driven, the present natural convection flow is driven by the thermal boundary layers at the interfaces. Hence, the flowfield is inherently more sensitive to the heat transfer conditions at the interfaces (especially at the source) that can be easily perturbed by radiation.

To study the effects of radiation, we again first look at the wall temperature distributions. It is evident from Fig. 8 that in the absence of radiation, $Nr \rightarrow 0.0$, there is a considerable difference between the temperatures of the convectively heated top wall and the convectively cooled bottom wall. At $Nr = 10$, however, as a result of significant radiative heating by the source and radiative exchange with the top wall, the temperture of the bottom wall is considerably increased. At the boundaries, radiative transfer is balanced by convection; therefore the bottom wall imparts the heat delivered by radiation to the cold fluid above it. A comparison between the temperature contours in Figs. 7 and 9 clearly indicates that in the $Nr = 10$ case, because of this heating by the bottom wall, the axial temperature gradients in the vicinity of the bottom

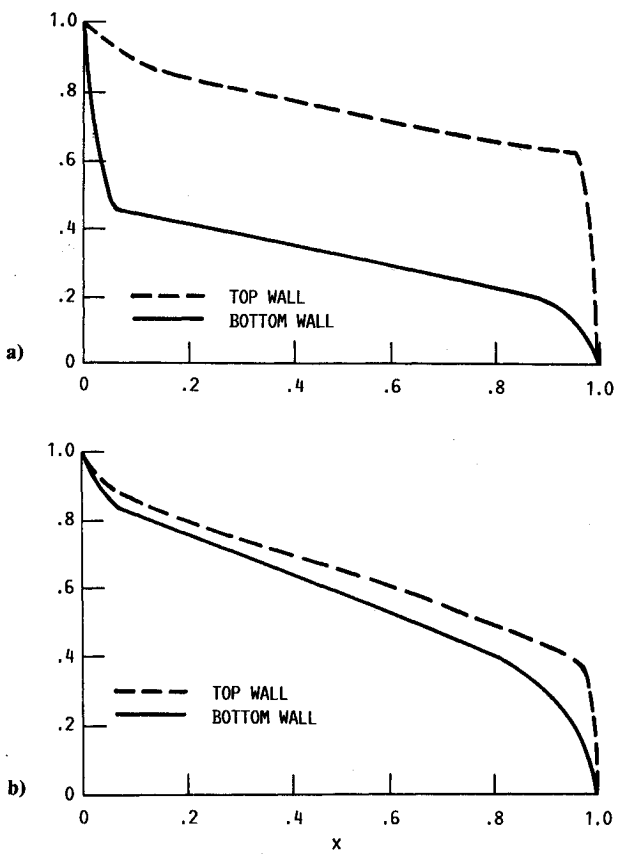

Fig. 8 Wall temperature distribution for $Gr = 1 \times 10^5$; a) no radiation, $Nr \rightarrow 0.0$; b) radiation, $Nr = 10.0$.

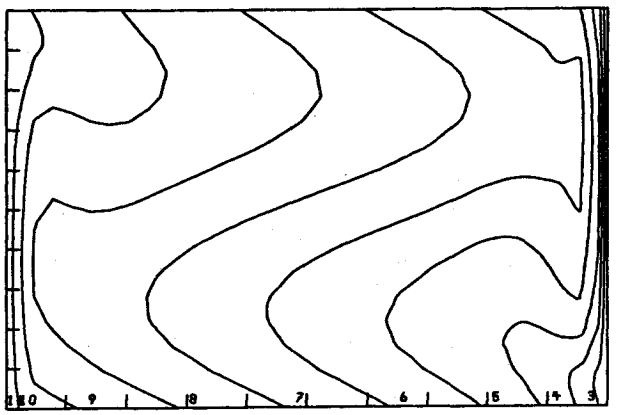

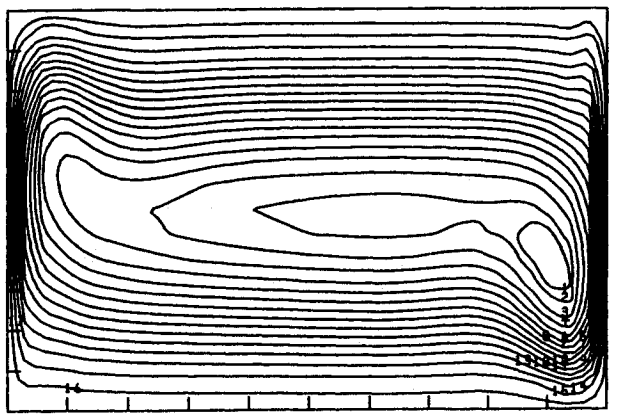

Fig. 9 Flow and temperature fields for combined convection and radiation heat transfer; $Gr = 1 \times 10^5$ and $Nr = 10$.

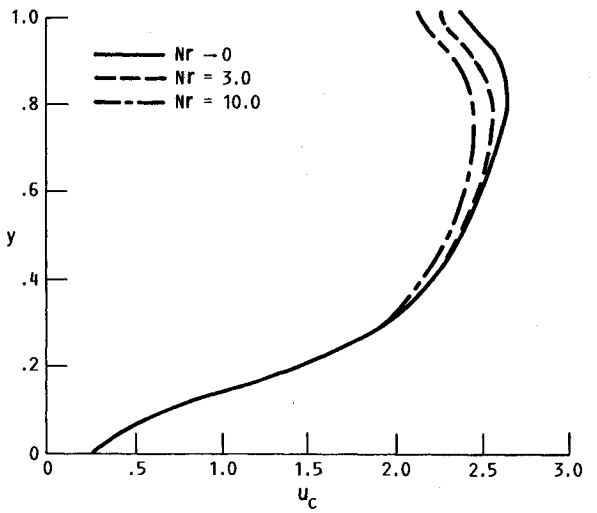

Fig. 10 Effect of the radiation-conduction number on the normal velocity distribution at the crystal interface for $Gr = 1 \times 10^5$.

wall and the source are noticeably relaxed. Consequently, as indicated by the stream function distribution in Fig. 9, radiative transfer indirectly weakens the flow near the source. Our numerical results show that for $Gr = 3 \times 10^4$ and $Nr = 10$ when convection is weaker, radiation effects can almost eliminate the vortex near the source.

The net effect of these interactions on the velocity distribution at the crystal interface for $Gr = 1 \times 10^5$ is shown in Fig. 10. Note that in comparison to $Gr = 700$ case, Fig. 5, the nonuniformity in the interfacial velocity u_c is substantial (Figs.

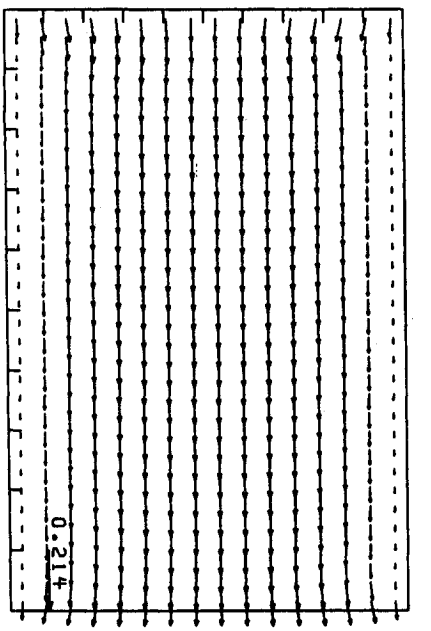

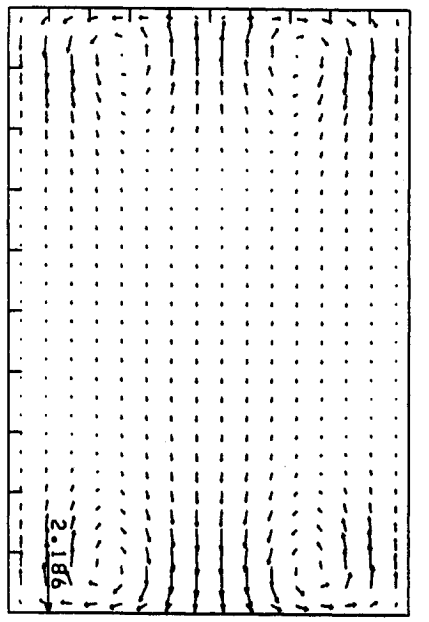

Fig. 11 Flowfield for the top-heated vertical cavity ($Gr = 1 \times 10^4$, $\gamma = 0.90$); a) no radiation, $Nr \to 0.0$; b) radiation, $Nr = 50$.

5 and 10 have different scales). Furthermore, note that as the effect of radiation increases with increasing Nr, because of the weakening of the flow near the source and the inherent sensitivity of the boundary-layer-driven flow to this effect, the supply of nutrients to the crystal is decreased, leading to a decline in the growth flux in the upper portion of the interface.

Vertical Enclosure

Another case in which the complicating action-at-a-distance nature of radiation is exemplified is the vertical or so-called stable configuration. In particular, we consider the case where the source is on top and the crystal forms the bottom boundary. This time we are considering a situation where the temperature difference is small; therefore $\gamma = 0.90$. But Nr is rather large and equal to 50. It is clear that in this top-heated enclosure, if radiative effects are neglected, convection currents are also absent. Conduction is the mode of heat transfer

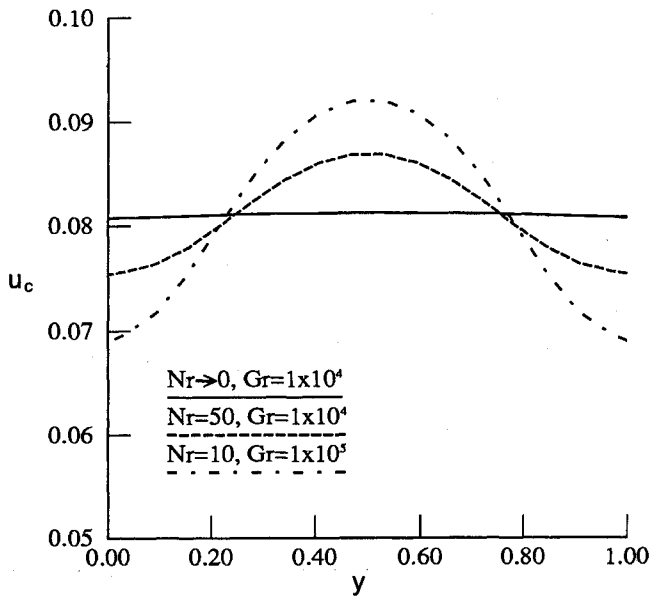

Fig. 12 Effect of the radiation-conduction number on the normal velocity distribution at the crystal interface for the top-heated vertical cavity, $\gamma = 0.90$.

in the vapor, and in the absence of buoyancy-driven convection as shown in Fig. 11a, a diffusive advective flow transports the nutrient from the source to the crystal. Although due to wall frictional effects the vapor is pushed toward the center of the enclosure at the source and expands outward at the sink, in the major portion of the cavity the mass average velocity profile is basically parabolic and unidirectional. Also note that since mass average velocity goes to zero at the walls, component *B* must recirculate in the enclosure as has been previously discussed in Ref. 4. Finally, Fig. 12 indicates that although the mass average flow produces an almost uniform velocity at the interface, because of the retarding effect of wall friction the interfacial velocity is slightly reduced near the wall. It should be mentioned that if the diffusive advective flow is strong, it can set up transverse temperature gradients that can induce convection. This has been indicated by Markam and Rosenberger[6] for a compressible flow. They have shown a distortion of the parabolic velocity profile by convection caused by transverse temperture gradients. In what follows, we will show that because of radiation heat transfer the top-heating configuration becomes convectively unstable, resulting in drastic alteration of the flowfield.

In the presence of surface radiation, the stable situation is disrupted. The insulated side walls that are heated by radiation deliver this heat to the cold fluid near the crystal interface. Temperature gradients are set up, and as shown in Fig. 11b, the fluid is forced to rise until it loses momentum and is carried down by the Stefan wind. The buoyancy fields created in the vicinity of the side walls and the crystal give rise to a symmetrical flow pattern that is clearly discerned in Fig. 11 for $Gr = 1 \times 10^4$. At this *Gr* number, the vortices near the crystal are so strong that the shear flow caused by them results in two weak counter-rotating vortices in the upper portion of the enclosure. As a result of this radiation-induced flow pattern, the flux of nutrient into the crystal is no longer uniform. As illustrated in Fig. 12, for these cases the maximum interfacial flux occurs at the center of the crystal interface where the flow is reinforced by the recirculation pattern and the minimum flux is near the side walls where buoyancy-driven flow opposes the supply of nutrients. The extent of the nonuniformity in the growth flux depends on the magnitude of *Gr* and *Nr*. It is evident that for lower *Gr* the u_c distribution is more uniform. Similarly, our numerical results predict a decrease in the nonuniformity of the interfacial flux at lower *Nr* values when radiation effects are less important.

Conclusions

The interaction between surface radiation and thermal convection in a vapor phase crystal growth enclosure was studied numerically. The transport process was found to be significantly affected by an intricate interplay between conduction, convection, and radiation. Based on a systematic parametric study, the complicating effects of thermal radiation were delineated to be as follows.

1) Ground-based applications usually involve high *Gr* numbers. In these convection-dominated situations our results for the horizontal enclosure indicate that the effects of surface radiation are manifested by a weakening of the boundary-layer-driven flow near the source that decreases the supply of nutrients to the upper portion of the growing crystal.

2) There is also considerable commercial interest in growing crystals in the microgravity environment of space where convection is minimized. It is therefore imperative to recognize that in low *g*, radiation only has to compete with conduction and can easily become the dominant heat transfer mode. Numerical simulations indicate that in this situation, due to the effects of passive radiation, a vigorous vortex is created near the interface that significantly increases the nonuniformity in the flux of nutrients to the crystal.

3) In many instances, the top-heating configuration is used to minimize convection. Our results, however, show that in the presence of radiation and for high to moderate Grashof numbers, the top-heating configuration is no longer stable, and radiation-induced vortices introduce significant nonuniformities in the crystal growth flux.

4) The shape and stability of the interface is closely related to temperature gradients near the interface. Our results clearly indicate that these temperature gradients are drastically affected by radiation. Therefore, radiative heat transfer may have a considerable influence on the shape and stability of the interface. Incorporation of these effects was, however, outside the scope of the present work.

Finally, throughout this work, the inherent sensitivity of vapor transport to wall temperature distributions and temperature gradients was emphasized. In many crystal growth experiments, the axial temperature distribution is imposed by external radiative heaters. In this situation, correct wall temperatures can only be computed through a conjugated heat transfer analysis. In this study, we neglected participation of the vapor in radiative transfer, which also can alter the temperature gradients. The assumptions of constant thermophysical properties and Boussinesq approximation are idealizations that should be relaxed in future studies, especially when large temperature gradients are present. We still hope that our results help in understanding the nature of the radiation effects and in isolating them from convection during crystal growth from the vapor phase.

References

[1]Wiedemeier, H., Klaessig, F. C., Irene, E. A., and Wey, S. J., "Crystal Growth and Transport Rates of GeSe and GeTe in Micro-Gravity Environment," *Journal of Crystal Growth*, Vol. 31, Dec. 1975, pp. 153–159.

[2]Rosenberger, F., "Fluid Dynamics in Crystal Growth from Vapors," *Physico-Chemical Hydrodynamics*, Vol. 1, No. 1, 1980, pp. 3–26.

[3]Klosse, K., and Ullersma, P., "Convection in a Chemical Vapor Transport Process," *Journal of Crystal Growth*, Vol. 18, No. 2, 1973, pp. 167–174.

[4]Greenwell, D. W., Markham, B. L., and Rosenberger, F., "Numerical Modelling of Diffusive Physical Vapor Transport in Cylindrical Ampoules," *Journal of Crystal Growth*, Vol. 51, No. 3, 1981, p. 413–425.

[5]Jhaveri, B. S., and Rosenberger, F., "Expansive Convection in Vapor Transport Across Horizontal Rectangular Enclosures," *Journal of Crystal Growth*, Vol. 57, No. 1, 1982, pp. 57–64.

[6]Markham, B. L., and Rosenberger, F., "Diffusive Convective Vapor Transport across Horizontal and Inclined Rectangular Enclosure," *Journal of Crystal Growth*, Vol. 67, No. 1, 1984, pp. 241–254.

[7]Extremet, G. P., Roux, B., Bontoux, P., and Elie, F., "Two-Dimensional Model for Thermal and Solutal Convection in Multizone Physical Vapor Transport," *Journal of Crystal Growth*, Vol. 82, No. 4, 1987, pp. 761-775.

[8]Zappoli, B., "Interaction Between Convection and Surface Reactions in Physical Vapor Transport in Rectangular Horizontal Enclosure," *Journal of Crystal Growth*, Vol. 76, No. 2, 1986, pp. 449-461.

[9]Yang, K. T., "Numerical Modeling of Natural Convection-Radiation Interactions in Enclosures," *Heat Transfer 1986,* Hemisphere, Washington, DC, 1986, pp. 131-140.

[10]Rosenberger, F., and Muller, G., "Interfacial Transport in Crystal Growth, A Parametric Comparison of Convective Effects," *Journal of Crystal Growth*, Vol. 65, No. 1-3, 1983, pp. 91-104.

[11]Wong, H. H., and Raithby, G. D., "Improved Finite-Difference Methods Based on a Critical Evaluation of The Approximation Errors," *Numerical Heat Transfer*, Vol. 2, 1979, pp. 139-163.

[12]Leonard, B. P., "A Convectively Stable, Third Order Finite Difference Method for Steady Two-Dimensional Flow and Heat Transfer," *Numerical Properties and Methodologies in Heat Transfer*, edited by T. M. Smith, Hemisphere, Washington, DC, 1983, pp. 211-226.

[13]Hottel, H. C., and Sarofim, A. F., *Radiative Transfer*, McGraw-Hill, New York, 1967.

[14]Kassemi, M., and Chung, B. T. F., "Conjugated Heat Transfer of Radiatively Participating Gas in a Channel," *Heat Transfer 1986*, Hemisphere, Washington, DC, 1986, pp. 797-802.

[15]De Vahl Davis, G., "Natural Convection of Air in a Square Cavity: A Bench Mark Numerical Solution," *International Journal of Numerical Methods Fluids*, Vol. 3, 1983, pp. 249-264.